ARTICLE

https://doi.org/10.1038/s41586-019-1278-0

Atypical behaviour and connectivity in *SHANK3*-mutant macaques

Yang Zhou[1,2,12,13], Jitendra Sharma[3,4,5,6,13], Qiong Ke[7,8,13], Rogier Landman[2,9,13], Jingli Yuan[10], Hong Chen[7], David S. Hayden[11], John W. Fisher III[11], Minqing Jiang[1], William Menegas[2], Tomomi Aida[2], Ting Yan[1], Ying Zou[1], Dongdong Xu[1], Shivangi Parmar[2,3], Julia B. Hyman[2,3], Adrian Fanucci-Kiss[2,3], Olivia Meisner[2,3], Dongqing Wang[2,3], Yan Huang[10], Yaqing Li[10], Yanyang Bai[1], Wenjing Ji[1], Xinqiang Lai[7], Weiqiang Li[7,8], Lihua Huang[7], Zhonghua Lu[1], Liping Wang[1], Sheeba A. Anteraper[2,3], Mriganka Sur[3,4,5], Huihui Zhou[1]*, Andy Peng Xiang[7,8]*, Robert Desimone[2,3], Guoping Feng[2,3,9]* & Shihua Yang[10]*

Mutation or disruption of the SH3 and ankyrin repeat domains 3 (*SHANK3*) gene represents a highly penetrant, monogenic risk factor for autism spectrum disorder, and is a cause of Phelan–McDermid syndrome. Recent advances in gene editing have enabled the creation of genetically engineered non-human-primate models, which might better approximate the behavioural and neural phenotypes of autism spectrum disorder than do rodent models, and may lead to more effective treatments. Here we report CRISPR–Cas9-mediated generation of germline-transmissible mutations of *SHANK3* in cynomolgus macaques (*Macaca fascicularis*) and their F1 offspring. Genotyping of somatic cells as well as brain biopsies confirmed mutations in the *SHANK3* gene and reduced levels of SHANK3 protein in these macaques. Analysis of data from functional magnetic resonance imaging revealed altered local and global connectivity patterns that were indicative of circuit abnormalities. The founder mutants exhibited sleep disturbances, motor deficits and increased repetitive behaviours, as well as social and learning impairments. Together, these results parallel some aspects of the dysfunctions in the *SHANK3* gene and circuits, as well as the behavioural phenotypes, that characterize autism spectrum disorder and Phelan–McDermid syndrome.

SHANK3 encodes major scaffolding proteins at excitatory synapses, coordinates the recruitment of signalling molecules and creates scaffolds for appropriate alignment of glutamatergic neurotransmitter receptors, which promotes the development and maturation of excitatory synapses[1,2]. Mutation of *SHANK3* accounts for about 1% of idiopathic forms of autism spectrum disorder, and disruption of *SHANK3* is a major cause of neurodevelopmental deficits in Phelan–McDermid syndrome[3–6]. Patients with a *SHANK3* gene mutation often exhibit a variety of comorbid traits, which include global developmental delay, severe sleep disturbances, lack of speech or severe language delay, and characteristic features of autism spectrum disorder (such as social impairments and stereotypies)[7–9]. Previous studies in flies, fish and rodents have uncovered impaired synaptic function and several behavioural abnormalities due to loss of SHANK3[2,10,11]. For example, common abnormalities in *Shank3*-mutant mice include self-injury, repetitive grooming, reduced interaction with conspecifics, motor difficulties and increased levels of anxiety. However, it is increasingly apparent that the validity of *Shank3*-mutant rodent models for human patients is limited, in part owing to the fact that the aberrant behavioural phenotypes in mice are found almost exclusively in homozygous mutants and are barely detectable in heterozygous mutants[2,12]. In addition, social interactions between humans involve integrated cognition and comprehension, which are more closely associated in primates than in rodents[13–16]. There is therefore an urgent need to develop primate models of autism spectrum disorder to facilitate neurobiological studies and the development of therapies[12,13,17].

Cynomolgus monkeys (*M. fascicularis*) possess a high level of cognitive ability and complex social behaviour, and are closer to humans in terms of their brain structure and function than are rodents[12,13,16,17]. There has been great interest in using macaques as a non-human-primate model for studying brain disorders[17–20]. Recent advances in CRISPR–Cas9-mediated gene-editing technology have resulted in an increasingly efficient and reliable method for targeted gene disruption, which is highly suited to the creation of non-human-primate models of autism spectrum disorder[21,22]. Previous attempts to create a transgenic *SHANK3* macaque model have been hindered by the early death of the mutant founders[23], or by the fact that only a single mutant survived[24]—group comparisons are not possible with only a single mutant. A viable primate model of *SHANK3* mutation should include validation of the loss of protein isoforms, and functional and behavioural deficits should be present at the group level. Furthermore, germline transmission of CRISPR–Cas9-edited macaque genomes has yet to be fully demonstrated. Here we report the creation of a *SHANK3*-mutant macaque model with a specific target locus that—in human studies—has been linked to Phelan–McDermid syndrome and autism spectrum disorder. We also demonstrate the resultant functional and behavioural abnormalities using assays that can be adapted for testing with autism spectrum disorder and Phelan–McDermid syndrome in human patients. Furthermore, we successfully obtained an

[1]Brain Cognition and Brain Disease Institute, Shenzhen Institutes of Advanced Technology, Chinese Academy of Sciences, Shenzhen, China. [2]McGovern Institute for Brain Research, Massachusetts Institute of Technology, Cambridge, MA, USA. [3]Department of Brain and Cognitive Sciences, Massachusetts Institute of Technology, Cambridge, MA, USA. [4]Picower Institute for Learning and Memory, Massachusetts Institute of Technology, Cambridge, MA, USA. [5]Simons Center for the Social Brain, Massachusetts Institute of Technology, Cambridge, MA, USA. [6]Athinoula A. Martinos Center for Biomedical Imaging, Department of Radiology, Massachusetts General Hospital, Charlestown, MA, USA. [7]Center for Stem Cell Biology and Tissue Engineering, Key Laboratory for Stem Cells and Tissue Engineering, Sun Yat-Sen University, Guangzhou, China. [8]Guangzhou Regenerative Medicine and Health Guangdong Laboratory, Guangzhou, China. [9]Stanley Center for Psychiatric Research, Broad Institute of MIT and Harvard, Cambridge, MA, USA. [10]College of Veterinary Medicine, South China Agricultural University, Guangzhou, China. [11]Computer Science and Artificial Intelligence Laboratory, Massachusetts Institute of Technology, Cambridge, MA, USA. [12]Present address: Montreal Neurological Institute & Hospital, Department of Neurology and Neurosurgery, McGill University, Montreal, Quebec, Canada. [13]These authors contributed equally: Yang Zhou, Jitendra Sharma, Qiong Ke, Rogier Landman. *e-mail: hh.zhou@siat.ac.cn; xiangp@mail.sysu.edu.cn; fengg@mit.edu; yangsh@scau.edu.cn

F1 generation that has a homogenous pattern of *SHANK3* mutation, using sperm from CRISPR-edited founders.

Germline-transmissible *SHANK3* mutation in macaques

We applied a CRISPR–Cas9 strategy that targets exon 21 of the macaque *SHANK3* gene (Extended Data Fig. 2a). Exon 21 is the largest coding region of *SHANK3*, with numerous rare variants and point mutations in individuals with autism spectrum disorder[2–5,7]. We created indels in exon 21 analogous to the human autism spectrum disorder-linked InsG3680 mutation[25] that were previously generated and analysed in mice[26,27]. *Streptococcus pyogenes* Cas9 and two guide (g)RNAs were introduced to generate the mutation, and the successful creation of insertions or deletions (indels) were verified (Extended Data Fig. 2b, c). We transferred injected embryos into recipient females, and obtained five live newborns (labelled M1 to M5) that carried *SHANK3* mutations (Extended Data Fig. 2d). Four out of the five mutants (M1, M2, M3 and M5) are male, and one mutant (M4) is female. Genotyping of *SHANK3* from the newborns revealed several types of indel mutations in the *SHANK3* gene (Fig. 1a, Extended Data Fig. 3). M2 and M5 did not show a wild-type allele in genomic DNA; they are homozygous and compound-heterozygous, respectively (Fig. 1a, Extended Data Fig. 3). M1, M3 and M4 carried wild-type alleles in about 50% of the sequenced clones and thus are heterozygous, with (M1 and M3) or without (M4) genetic mosaicism (more than one type of indel). The control group consisted of age- and sex-matched macaques from the same colony. The general health measurements of the *SHANK3*-mutant macaques (such as body weight) were not different from controls (Extended Data Fig. 2e). Body condition scores of control and mutant groups were within the normal range for this species.

Sequencing results in exon 21 of the *SHANK3* gene showed multiple genotypes, which suggests that the CRISPR–Cas9-mediated cleavage of *SHANK3* resulted in a mosaicism of indels, as has previously been reported[21,22]. All of the indels from *SHANK3* mutants caused frameshift and loss-of-function mutations, except for a 12-bp in-frame deletion in mutant M4 and a 96-bp deletion in mutant M3; these led to a loss of 4 and 32 amino acids, respectively, within the proline-rich domain of SHANK3, which might be critical for the stability of SHANK3 protein isoforms and their interaction with scaffolds or receptors[1,2,7]. To determine how mutations of *SHANK3* affected the protein products of this gene, we biopsied tissue from primary visual cortex and performed western blot analysis. The biopsies were performed after completion of all behavioural tests and magnetic resonance imaging (MRI) scanning. We confirmed a decreased level of the isoforms of the SHANK3 protein in all five mutant monkeys (Fig. 1b, c, Extended Data Figs. 1 and 4) and thus validated the successful targeted disruption of exon 21, which has previously been linked to synaptic and circuit dysfunction[2,11,26,27].

To test for off-target modifications, we amplified and sequenced the top 20 genomic loci that were predicted by the Cas-OFFinder algorithm[28]. We analysed the sequencing results of these 20 loci from all 5 *SHANK3* mutants and confirmed their wild-type identities (Supplementary Table 1). Our data support the high fidelity of gene editing with CRISPR–Cas9, which aligns with previous surveys of CRISPR-edited model organisms[22].

To assess the germline transmission of the mutation, we collected and analysed the DNA of sperm from M2 (homozygous) and M3 (heterozygous and mosaic). We detected *SHANK3* mutations in the DNA of sperm cells of both individuals, and the patterns of mutation were similar to their respective somatic cells (Fig. 1d, Extended Data Figs. 1, 2f). We then performed intracytoplasmic sperm injection into wild-type oocytes using semen from monkey M2 (homozygous), and detected a 40-bp deletion mutation in all fertilized embryos (Fig. 1e, Extended Data Fig. 1). We successfully obtained live births of F1-generation mutant macaques after transferring the fertilized embryos. Genotyping of F1-generation mutant monkeys from the first cohort (labelled F1-1, F1-2 and F1-3) revealed a similar ratio of wild-type to mutant allele (labelled 'del 40 bp') from all three monkeys (Fig. 1f, Extended Data Fig. 1), which indicates that these are heterozygous *SHANK3*-mutant monkeys without genetic mosaicism. Taken together, these results show that the simultaneous delivery of two gRNAs that target both strands of exon 21 enables the efficient mutagenesis of *SHANK3* and the germline transmission of the mutant allele, in cynomolgus monkeys.

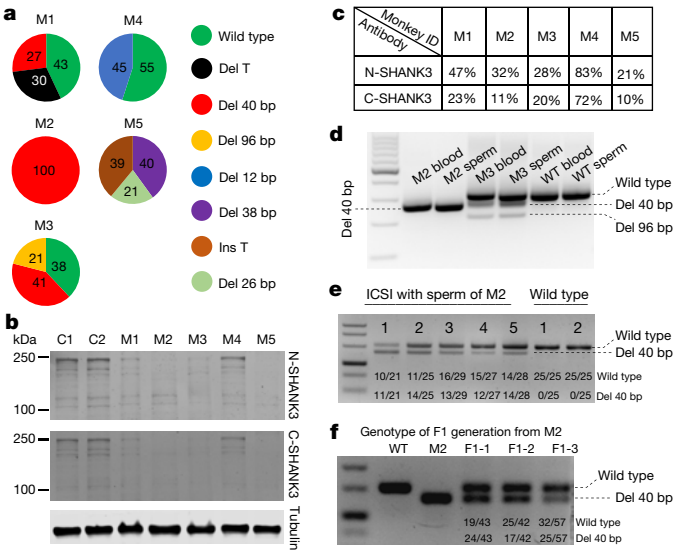

Fig. 1 | Generation and germline transmission of macaques with *SHANK3* mutations. a, Pie charts of genotype (indels) from cultured skin fibroblasts derived from each mutant monkey. **b**, Representative western blots using brain lysates prepared from a V1 biopsy of two wild-type macaques (labelled C1 (male) and C2 (female)) and all five mutants (M1–M5), probed with N-terminal and C-terminal antibodies, and α-tubulin as loading control on the same gel. **c**, Relative levels of SHANK3 proteins calculated by averaging five technical repeats with the same V1 biopsy sample, and normalizing to α-tubulin loading controls. **d**, Genotyping PCR results of *SHANK3* from DNA from blood and sperm samples collected from M2, M3 and a wild-type (WT) control. **e**, Top, genotyping PCR results of *SHANK3* from individual cultured embryos after intracytoplasmic injection of single sperm (ICSI) from M2 and a wild-type control. Bottom, numbers of reads for wild-type and a 40-bp deletion are presented by Sanger sequencing of each bacterial colony after cloning of PCR products into sequencing vector. **f**, Top, genotyping PCR results of three live-birth, F1-generation monkeys after ICSI of sperm from M2. Bottom, numbers of reads for wild-type and a 40-bp deletion for each monkey (F1-1, F1-2 and F2-3) by Sanger sequencing of cloned PCR products.

Altered sleep, home cage activity and muscle tone

Patients with Phelan–McDermid syndrome and other individuals with *SHANK3* mutations often exhibit a variety of traits, which include motor impairment, severe sleep disturbances, lack of speech or severe language delay, abnormal sensory processing, intellectual disability, muscular hypotonia and seizure, as well as other symptomologies[2–8]. Most patients with Phelan–McDermid syndrome also exhibit stereotypies, and impairments in social interaction[4,8]. We used a panel of behavioural tests to examine phenotypes associated with *SHANK3* mutation in macaques. All observations, scoring and data analysis for these tests were carried out by researchers who were blinded to experimental design, goals and genotypes.

To assess sleep disturbance in the mutant monkeys, we habituated them to wearing an actigraphy device. The activity data revealed that overall activity levels were substantially reduced in mutant monkeys compared to controls (Fig. 2a–g). Mutant monkeys displayed a longer latency to sleep than controls, and an increased frequency of waking (as indicated by a fragmentation index) (Fig. 2h, i). These results showed a reduction in overall sleep efficiency in *SHANK3*-mutant monkeys (Fig. 2j, Extended Data Fig. 5).

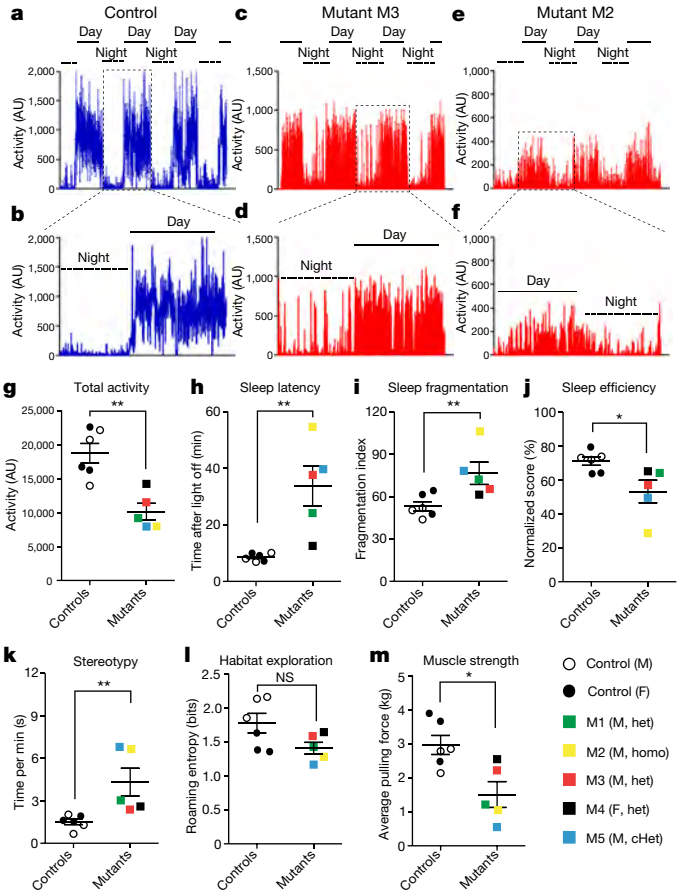

Fig. 2 | Sleep disturbances and altered home-cage activity in *SHANK3*-mutant macaques. a, **c**, **e**, Representative traces of overall activity recorded by a motion watch across multiple days from a control macaque and two mutants. AU, arbitrary units. **b**, **d**, **f**, Enlarged traces of overall activity recorded by motion watch over the course of 24 h from a control macaque, M3 and M2. **g**, Reduced overall activity in *SHANK3* mutants. **h**, Increased latency to fall asleep in *SHANK3* mutants. **i**, Increased fragmentation of sleep in *SHANK3* mutants during the night. **j**, Reduced efficiency of sleep in *SHANK3* mutants during the night. **k**, Increased time spent on stereotypic behaviours, presented as seconds per minute, in *SHANK3* mutants. **l**, *SHANK3* mutants show a trend of reduced area exploration in their home cages, as defined by roaming entropy. **m**, *SHANK3* mutants display reduced muscle strength. In **g**–**m**, $n = 6$ macaques for control group; $n = 5$ macaques for the *SHANK3*-mutant group; P value = 0.0087 (**g**), 0.0043 for (**h**), 0.0087 (**i**), 0.0303 (**j**), 0.0043 (**k**), 0.08 (**l**) and 0.03 (**m**). Data are presented as mean ± s.e.m. Two-tailed Mann–Whitney *U*-test. Coloured squares indicate individual monkeys with *SHANK3* mutation. M, male; F, female, het, heterozygous; homo, homozygous; cHet, compound heterozygous.

We recorded daily home-cage videos and scored behavioural variables using Noldus Observer software (see representative ethograms in Supplementary Table 2). The mutant macaques showed a substantial increase in stereotyped or repetitive behaviours compared to controls, as indicated by increased back-flipping, finger licking and biting of cage bars (Fig. 2k). In contrast to the increased amount of self-injurious grooming that is consistently observed in *Shank3*-mutant mice, the stereotypy in *SHANK3*-mutant monkeys was diverse. For instance, repetitive flipping was observed in mutant M3, whereas M2 and M5 displayed a pronounced licking of fingers and cage bars. The mutant macaques also displayed a trend for reduced level of exploration of cage subdivisions, as demonstrated by roaming entropy (Fig. 2l).

To test for hypotonia, we habituated the monkeys to pull a digital scale and recorded their pulling force. The average pulling force was reduced in the mutant group (Fig. 2m).

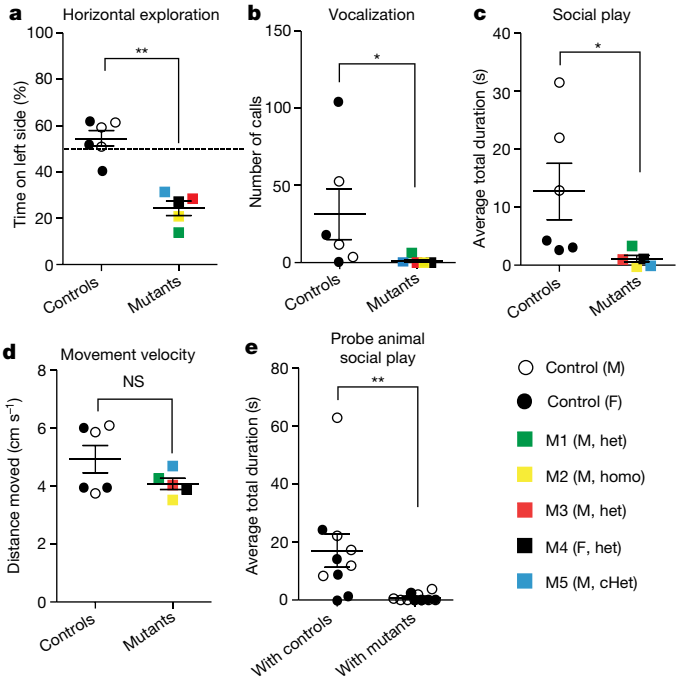

Fig. 3 | Impaired social interaction and reduced vocalization in *SHANK3* mutants. a, Proportion of time spent on the left versus right side of the cage shows that mutants tended to stay on one side, whereas control monkeys spent a roughly equal amount of time on each side. **b**, *SHANK3*-mutant monkeys made fewer vocalizations during the habituation period than did controls. **c**, Average total duration of aggregate social behaviours (which included chasing, following, fleeing, circling and play) was lower in mutants than in controls. **d**, No difference in movement velocity during the social test between mutants and controls. **e**, Average total duration of aggregate social behaviours was reduced in probe monkeys (wild type) when paired with *SHANK3* mutants, compared to probe monkeys paired with controls. $n = 6$ macaques for wild-type control group; $n = 5$ macaques for *SHANK3*-mutant group; in **e**, $n = 10$ wild-type macaques (five males, five females and age-matched to experimental animals) for probe monkeys. $P = 0.0043$ (**a**), 0.0444 (**b**), 0.0173 (**c**) and 0.0023 (**e**). NS, not significant. Data are presented as mean ± s.e.m. Two-tailed Mann–Whitney *U*-test. Coloured squares indicate individual monkeys with *SHANK3* mutation.

Impaired social interaction

We designed a paired social interaction assay between juvenile monkeys. The monkeys were habituated in the test cage before the social test began (Extended Data Fig. 6a). During habituation, the mutant macaques showed a reduced amount of exploration in the horizontal plane (Fig. 3a). Vocalization during the 20 minutes of habituation was reduced in the mutants (Fig. 3b). In the social interaction test, the scoring of detailed activities for the first five minutes revealed that mutants spent less time on aggregate social behaviours, which included chasing, following, circling, fleeing and play (Fig. 3c, Extended Data Fig. 6b–f). The mean velocity values during the social interactions were similar between the mutant and control monkeys (Fig. 3d), which suggests that physical limitations were unlikely to be major contributing factors to the reduced levels of social interaction. Furthermore, there was no difference in time spent on other categories of behaviours, such as attacking, anogenital inspection, rump presentation, mounting, and receiving and giving grooming during the social test (Extended Data Fig. 6g–l). The aggregate social behaviour values decreased in the subsequent five minutes for the control group, and approached that of the mutant monkeys (Extended Data Fig. 6m). Analysing the behaviours of the wild-type probe monkeys (that is, the monkeys with which the mutant and control groups interacted) during the same time period revealed notable differences between pairings with wild-type controls and the *SHANK3* mutants. In aggregate measures, the probe monkeys

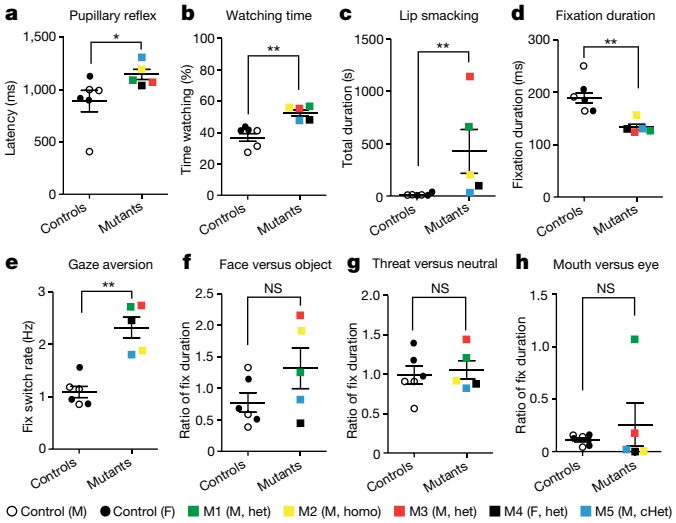

Fig. 4 | Eye-tracking properties in *SHANK3*-mutant macaques. **a**, Latency of pupillary reflex upon stimuli illuminance is increased in *SHANK3* mutants. **b**, Percentage of time watching the screen is increased in *SHANK3* mutants. **c**, *SHANK3* mutants display increased lip smacking when watching the video presentation of close-up and whole-body videos of monkeys. **d**, The duration of each fixation during the presentation of images was reduced in *SHANK3* mutants. **e**, Increased fixation-switch rate in *SHANK3* mutants. **f**–**h**, No difference in the ratio of fixation duration in face versus object (**f**), threat versus neutral faces (**g**) or mouth versus eye region (**h**) from macaques tested with image stimuli. NS, not significant. $n = 6$ macaques for control group; $n = 5$ macaques for mutant group. $P = 0.0303$ (**a**), 0.0043 (**b**), 0.0043 (**c**), 0.008 (**d**) and 0.0043 (**e**). Data are presented as mean ± s.e.m. Two-tailed Mann–Whitney *U*-test. Coloured squares indicate individual monkeys with *SHANK3* mutation.

spent less time playing with the *SHANK3* mutants than they did playing with the controls (Fig. 3e, Extended Data Fig. 7a–k). The differential effects on probe monkeys are reminiscent of the effects of oxytocin and vasopressin application on looking behaviour in macaques[29]. These results suggest the *SHANK3*-mutant monkeys display reduced levels of exploration, social interaction and vocalization, which seem to parallel some aspects of the phenotypes that are found in humans with Phelan–McDermid syndrome or autism spectrum disorder.

Altered gaze properties

We designed a video-based eye-tracking assay to investigate differences in gaze between control and mutant monkeys[30,31]. The mutants showed an increased latency of pupillary reflex to the onset of luminance at the start of the video stimulus (Fig. 4a), which is consistent with previous reports of delayed pupil reflex in humans with autism spectrum disorder[32]. The mutant monkeys spent more time watching both social and non-social videos than did controls (Fig. 4b). However, during the presentation of close-up and whole-body videos, mutant monkeys displayed frequent lip smacking and teeth chattering, which could be an indication of increased levels of anxiety or fear in response to the appearance of a conspecific[33,34] (Fig. 4c). We also assessed eye movements while the monkeys viewed pairwise still images of macaque faces and objects, or faces with threating and neutral expression[35,36]. Across all images, the mean dwell time per fixation was reduced in the mutant group (Fig. 4d). There was an increased rate of switching fixations between the two images (Fig. 4e), but not in the ratio of total fixation time (Fig. 4f–h). It has also previously been shown that human children who later develop autism have shorter durations of fixation[37].

To evaluate the cognitive performance of mutant monkeys, we trained them to perform a visual discrimination task, a reversal task and a Hamilton search task[18]. Despite extensive training, mutants M2 and M5 failed to participate in the test—possibly owing to impaired motor coordination or cognitive deficits. In black–white discrimination and reversal tasks, the controls and remaining mutants (M1, M3 and M4) performed similarly (Extended Data Fig. 8). In a Hamilton search task with three phases (Extended Data Fig. 9a), mutant and control monkeys were similar in first phase. However, M3 did not improve in the second phase (Extended Data Fig. 9b) and in the third phase, M1 and M4 exhibited learning impairment (Extended Data Fig. 9c). A χ^2 test of the proportion of monkeys that met a criterion of being correct 75% of the time by the final day of testing revealed a difference between the six controls and three mutants (Extended Data Fig. 9d). These results suggest a possible impairment in the mutants in terms of their switching strategies across the phases of Hamilton search; however, the small number of mutant monkeys that could perform the task prevent us from reaching a firm conclusion regarding the nature of their impairment.

Altered brain connectivity

MRI studies of individuals with autism spectrum disorder suggest that considerable structural and functional changes of the brain are associated with this disorder[38,39]. Structural MRI analysis in *SHANK3*-mutant monkeys revealed a decrease in grey matter but no difference in white matter and cerebrospinal fluid volumes, compared to those of controls (Extended Data Fig. 10a–c).

Altered functional connectivity has recently emerged as a possible biomarker for autism spectrum disorder[40–42]. We used an unbiased, data-driven, voxel-by-voxel, global and local functional correlation[43] (see Methods), and found that long-range connectivity between several brain regions in mutants was reduced relative to that in controls. Notably, we found that in mutants there was hypo-connectivity in putative default-mode networks, including the posterior cingulate cortex, medial prefrontal region and motor regions (Fig. 5a, d–f). We also identified local hypo-connectivity in thalamic and striatal regions (Fig. 5b, c, g, h) in the mutants. By contrast, we detected local hyper-connectivity in the somatosensory cortex, extrastriate cortical areas, and posterior cingulate cortex of the mutant monkeys (Fig. 5b, c, i, j). Seed-based analysis confirmed these results of reduced global connectivity and greater local connectivity in *SHANK3* mutants (Extended Data Fig. 10d–f). Taken together, our MRI data indicate that the mutant macaques have a dysregulated resting-state connectivity, both globally and locally.

Discussion

In this model of the *SHANK3* mutation in macaques, we observed a combination of reduced mobility, increased repetitive behaviours and impaired sociability that reconciles previous studies in rodents[2,11,26,27]. *SHANK3* mutants exhibit notable sleep disturbances and activity differences, which may assist in the discovery of characteristic biomarkers for Phelan–McDermid syndrome, autism spectrum disorder and other neurodevelopmental disorders in humans[38,44]. Altered social behaviours and stereotypy (such as licking fingers and cage bars), as well as reduced muscle strength and a lack of vocalization, in the *SHANK3*-mutant monkeys parallels the hypotonia and speech or language impairments of children with autism spectrum disorder or Phelan–McDermid syndrome[4,8]. An altered pupillary light reflex, such as we found in the mutant monkeys, has been reported in autism spectrum disorder[32]; this has not specifically been examined in Phelan–McDermid syndrome, and warrants further exploration. *SHANK3* mutants displayed comparable learning ability to controls in a simple visual discrimination task. However, a more-complex Hamilton search task revealed learning impairments that might arise from reduced flexibility or switching of strategies. Given that we could behaviourally test only a small number of mutants, further cognitive testing of larger groups will be needed to characterize any intellectual impairment.

Autism spectrum disorder is a heterogeneous disorder both in terms of the clinical manifestation of symptoms and its underlying aetiology. In fact, the genetic predisposition for autism spectrum disorder is likely to be different among individuals, even when the same gene is affected[3–9]. It is therefore difficult to draw general conclusions from a single mutant monkey (as recently reported[24]), owing to the

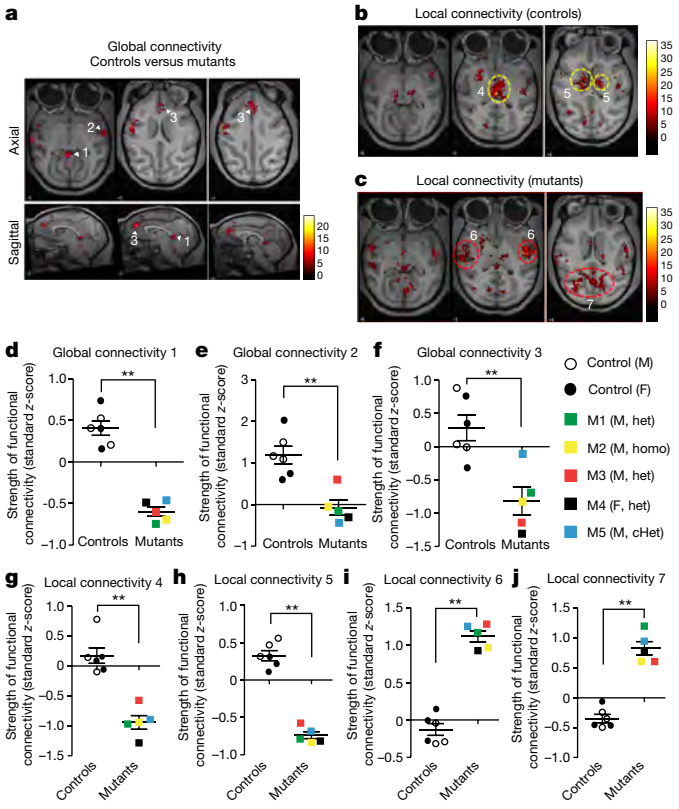

Fig. 5 | Dysregulated global and local connectivity in *SHANK3*-mutant macaques. a, Axial and sagittal views of differential global connectivity between control and mutant groups. Clusters with robustly higher global connectivity are highlighted by an arrowhead, and numbered. Putative brain regions are posterior cingulate cortex (1), motor cortex (2) and anterior cingulate cortex (3). **b**, **c**, Axial views of local connectivity in controls and mutants. Clusters with robust alteration of local connectivity are highlighted and numbered with dashed circles. Putative brain regions are thalamic regions (4), striatum (5), somatosensory cortex (6) and near the posterior cingulate cortex and extrastriate cortical areas (7). **d**–**f**, Normalized global connectivity shows a reduced strength in *SHANK3* mutants for regions 1, 2 and 3 (corresponding to **a**). **g**, **h**, Normalized local connectivity shows a reduced strength in *SHANK3* mutants for regions 4 and 5 (corresponding to **b**). **i**, **j**, Normalized local connectivity shows an increased strength in *SHANK3* mutants for regions 6 and 7 (corresponding to **c**). In **d**–**j**, $n = 6$ macaques for control group; $n = 5$ macaques for *SHANK3*-mutant group. $P = 0.0043$ (**d**), 0.0087 (**e**, **f**) and 0.0043 (**g**–**j**). Data are presented as mean ± s.e.m. Two-tailed Mann–Whitney *U*-test. Within-group threshold of $P < 0.001$ and $P < 0.05$ family-wise error correction of $P < 0.05$ (with a cluster-forming threshold of $k > 25$) were used. Coloured squares indicate individual monkeys with *SHANK3* mutation.

heterogeneity of symptoms that are related to this disorder, as well as the variability of personalities and abilities even in wild-type monkeys. Among the five founder *SHANK3*-mutant macaques, we observed considerable heterogeneity in the severity of behavioural manifestations, including motor impairments, stereotypies and learning problems in a complex task. Differential behavioural outcomes could result from normal inter-monkey variability, different mutation patterns in *SHANK3* and/or different genetic backgrounds owing to the monkeys being outbred. Among the five mutant monkeys, M4 is closer to the wild-type controls than are the other mutants for many behavioural variables (for example, total activity measure; Fig. 2g), which is consistent with its genotype and protein expression. M4 carries an in-frame deletion that causes a reduction in the levels of SHANK3 protein of about 20%; the level of reduction in SHANK3 protein isoforms is greater in the homozygous mutant (M2), the compound-heterozygous mutants (M1 and M5) and the heterozygous mutant (M3). Given the small number of monkeys in this study, as well as their genetic heterogeneity, all of our findings will need to be confirmed in larger numbers of monkeys in the future. Some of the genetic heterogeneity will be better controlled in F1-generation macaques.

In this initial characterization of *SHANK3* mutants, we are unable to pinpoint any of the causes that might underlie the behavioural differences. Anxiety disorder, exacerbated in a social context, could be a common contributor[45,46]. The hypoactivity and compromised general exploratory activity that we observed in *SHANK3*-mutant monkeys could contribute to the low reciprocity of social interactions and lack of vocalization, although the movement velocity of the mutants during the social tests did not differ from that of the controls. The altered structural MRI and neural connectivity measures may be immune to possible confounding factors. Clinical studies have shown that children and adults with sleep disorders are prone to develop language problems, and have compromised attention and executive function compared to healthy sleepers[44]. Autistic children with serious sleep disorders may have difficulty controlling repetitive behaviours, and may show a lower performance on tests of attention and memory[47]. The *SHANK3*-mutant monkeys provide an opportunity to test complex interactions such as these in the future.

Autism spectrum disorder is thought to affect multiple interconnected regions of the brain, and there is evidence for alterations in brain connectivity that could contribute to the behavioural phenotypes that are associated with autism spectrum disorder[39,48]. Recent studies have suggested that non-human primates have a resting-state default-mode network that is similar to that of humans[49,50]. Our discovery in a non-human-primate model of atypical connectivity in local and long-range circuits—especially in the cingulate, frontal, thalamic and striatal regions—suggests a path for further studies to identify circuit abnormalities and potential biomarkers for treatment studies. Monogenic forms of autism spectrum disorder may also offer insights into altered functional brain connectivity in polygenic or idiopathic autism spectrum disorder. Future longitudinal studies of resting-state functional connectivity, combined with in vivo recordings and circuit manipulations, in the second generation of *SHANK3*-mutant monkeys may allow for an in-depth understanding of the development of aberrant connectivity in neural circuits and their relevance for the behavioural phenotypes that characterize autism spectrum disorder.

Online content

Any methods, additional references, Nature Research reporting summaries, source data, statements of data availability and associated accession codes are available at https://doi.org/10.1038/s41586-019-1278-0.

Received: 4 November 2018; Accepted: 13 May 2019;
Published online 12 June 2019.

1. Naisbitt, S. et al. Shank, a novel family of postsynaptic density proteins that binds to the NMDA receptor/PSD-95/GKAP complex and cortactin. *Neuron* **23**, 569–582 (1999).
2. Jiang, Y. H. & Ehlers, M. D. Modeling autism by *SHANK* gene mutations in mice. *Neuron* **78**, 8–27 (2013).
3. Moessner, R. et al. Contribution of *SHANK3* mutations to autism spectrum disorder. *Am. J. Hum. Genet.* **81**, 1289–1297 (2007).
4. Phelan, K. & McDermid, H. E. The 22q13.3 deletion syndrome (Phelan–McDermid Syndrome). *Mol. Syndromol.* **2**, 186–201 (2012).
5. Betancur, C. & Buxbaum, J. D. SHANK3 haploinsufficiency: a "common" but underdiagnosed highly penetrant monogenic cause of autism spectrum disorders. *Mol. Autism* **4**, 17 (2013).
6. Sanders, S. J. et al. Insights into autism spectrum disorder genomic architecture and biology from 71 risk loci. *Neuron* **87**, 1215–1233 (2015).
7. Leblond, C. S. et al. Meta-analysis of SHANK mutations in autism spectrum disorders: a gradient of severity in cognitive impairments. *PLoS Genet.* **10**, e1004580 (2014).
8. Frank, Y. et al. A prospective study of neurological abnormalities in Phelan–McDermid syndrome. *J. Rare Disord.* **5**, 1–13 (2017).
9. Chen, J. A., Peñagarikano, O., Belgard, T. G., Swarup, V. & Geschwind, D. H. The emerging picture of autism spectrum disorder: genetics and pathology. *Annu. Rev. Pathol.* **10**, 111–144 (2015).
10. Gauthier, J. et al. De novo mutations in the gene encoding the synaptic scaffolding protein *SHANK3* in patients ascertained for schizophrenia. *Proc. Natl Acad. Sci. USA* **107**, 7863–7868 (2010).

11. Peça, J. et al. *Shank3* mutant mice display autistic-like behaviours and striatal dysfunction. *Nature* **472**, 437–442 (2011).
12. Jennings, C. G. et al. Opportunities and challenges in modeling human brain disorders in transgenic primates. *Nat. Neurosci.* **19**, 1123–1130 (2016).
13. Bauman, M. D. & Schumann, C. M. Advances in nonhuman primate models of autism: integrating neuroscience and behavior. *Exp. Neurol.* **299**, 252–265 (2018).
14. Chang, S. W. et al. Neuroethology of primate social behavior. *Proc. Natl Acad. Sci. USA* **110**, 10387–10394 (2013).
15. Platt, M. L., Seyfarth, R. M. & Cheney, D. L. Adaptations for social cognition in the primate brain. *Phil. Trans. R. Soc. Lond. B* **371**, 20150096 (2016).
16. Izpisua Belmonte, J. C. et al. Brains, genes, and primates. *Neuron* **86**, 617–631 (2015).
17. Sclafani, V. et al. Early predictors of impaired social functioning in male rhesus macaques (*Macaca mulatta*). *PLoS ONE* **11**, e0165401 (2016).
18. Liu, Z. et al. Autism-like behaviours and germline transmission in transgenic monkeys overexpressing MeCP2. *Nature* **530**, 98–102 (2016).
19. Chen, Y. et al. Modeling Rett syndrome using TALEN-edited MECP2 mutant cynomolgus monkeys. *Cell* **169**, 945–955 (2017).
20. Sasaki, E. et al. Generation of transgenic non-human primates with germline transmission. *Nature* **459**, 523–527 (2009).
21. Cong, L. et al. Multiplex genome engineering using CRISPR/Cas systems. *Science* **339**, 819–823 (2013).
22. Niu, Y. et al. Generation of gene-modified cynomolgus monkey via Cas9/RNA-mediated gene targeting in one-cell embryos. *Cell* **156**, 836–843 (2014).
23. Zhao, H. et al. Altered neurogenesis and disrupted expression of synaptic proteins in prefrontal cortex of *SHANK3*-deficient non-human primate. *Cell Res.* **27**, 1293–1297 (2017).
24. Tu, Z. et al. CRISPR/Cas9-mediated disruption of *SHANK3* in monkey leads to drug-treatable autism-like symptoms. *Hum. Mol. Genet.* **28**, 561–571 (2019).
25. Durand, C. M. et al. Mutations in the gene encoding the synaptic scaffolding protein SHANK3 are associated with autism spectrum disorders. *Nat. Genet.* **39**, 25–27 (2007).
26. Zhou, Y. et al. Mice with *Shank3* mutations associated with ASD and schizophrenia display both shared and distinct defects. *Neuron* **89**, 147–162 (2016).
27. Speed, H. E. et al. Autism-associated insertion mutation (InsG) of *Shank3* exon 21 causes impaired synaptic transmission and behavioral deficits. *J. Neurosci.* **35**, 9648–9665 (2015).
28. Bae, S., Park, J. & Kim, J. S. Cas-OFFinder: a fast and versatile algorithm that searches for potential off-target sites of Cas9 RNA-guided endonucleases. *Bioinformatics* **30**, 1473–1475 (2014).
29. Jiang, Y. & Platt, M. L. Oxytocin and vasopressin flatten dominance hierarchy and enhance behavioral synchrony in part via anterior cingulate cortex. *Sci. Rep.* **8**, 8201 (2018).
30. Falck-Ytter, T., Bölte, S. & Gredebäck, G. Eye tracking in early autism research. *J. Neurodev. Disord.* **5**, 28 (2013).
31. Mosher, C. P., Zimmerman, P. E. & Gothard, K. M. Videos of conspecifics elicit interactive looking patterns and facial expressions in monkeys. *Behav. Neurosci.* **125**, 639–652 (2011).
32. Daluwatte, C. et al. Atypical pupillary light reflex and heart rate variability in children with autism spectrum disorder. *J. Autism Dev. Disord.* **43**, 1910–1925 (2013).
33. Maestripieri, D. & Wallen, K. T. Affiliative and submissive communication in rhesus macaques. *Primates* **38**, 127–138 (1997).
34. Hinde, R. A. & Rowell, T. E. Communication by postures and facial expressions in the rhesus monkey (*Macaca mulatta*). *J. Zool.* **138**, 1–21 (1962).
35. Gothard, K. M., Battaglia, F. P., Erickson, C. A., Spitler, K. M. & Amaral, D. G. Neural responses to facial expression and face identity in the monkey amygdala. *J. Neurophysiol.* **97**, 1671–1683 (2007).
36. Parr, L. A. & Heintz, M. Facial expression recognition in rhesus monkeys, *Macaca mulatta*. *Anim. Behav.* **77**, 1507–1513 (2009).
37. Wass, S. V. et al. Shorter spontaneous fixation durations in infants with later emerging autism. *Sci. Rep.* **5**, 8284 (2015).
38. Tabet, A. C. et al. A framework to identify contributing genes in patients with Phelan–McDermid syndrome. *NPJ Genom. Med.* **2**, 32 (2017).
39. Rudie, J. D. et al. Altered functional and structural brain network organization in autism. *Neuroimage Clin.* **2**, 79–94 (2013).
40. Emerson, R. W. et al. Functional neuroimaging of high-risk 6-month-old infants predicts a diagnosis of autism at 24 months of age. *Sci. Transl. Med.* **9**, eaag2882 (2017).
41. Lewis, J. D., Theilmann, R. J., Townsend, J. & Evans, A. C. Network efficiency in autism spectrum disorder and its relation to brain overgrowth. *Front. Hum. Neurosci.* **7**, 845 (2013).
42. Buckner, R. L., Andrews-Hanna, J. R. & Schacter, D. L. The brain's default network: anatomy, function, and relevance to disease. *Ann. NY Acad. Sci.* **1124**, 1–38 (2008).
43. Whitfield-Gabrieli, S. & Nieto-Castanon, A. Conn: a functional connectivity toolbox for correlated and anticorrelated brain networks. *Brain Connect.* **2**, 125–141 (2012).
44. Goldman, S. E. et al. Defining the sleep phenotype in children with autism. *Dev. Neuropsychol.* **34**, 560–573 (2009).
45. Adolphs, R. The social brain: neural basis of social knowledge. *Annu. Rev. Psychol.* **60**, 693–716 (2009).
46. Arnsten, A. F. Stress signalling pathways that impair prefrontal cortex structure and function. *Nat. Rev. Neurosci.* **10**, 410–422 (2009).
47. Guénolé, F. et al. Melatonin for disordered sleep in individuals with autism spectrum disorders: systematic review and discussion. *Sleep Med. Rev.* **15**, 379–387 (2011).
48. Just, M. A., Keller, T. A., Malave, V. L., Kana, R. K. & Varma, S. Autism as a neural systems disorder: a theory of frontal-posterior underconnectivity. *Neurosci. Biobehav. Rev.* **36**, 1292–1313 (2012).
49. Moeller, S., Nallasamy, N., Tsao, D. Y. & Freiwald, W. A. Functional connectivity of the macaque brain across stimulus and arousal states. *J. Neurosci.* **29**, 5897–5909 (2009).
50. Vincent, J. L. et al. Intrinsic functional architecture in the anaesthetized monkey brain. *Nature* **447**, 83–86 (2007).

Acknowledgements We thank L. Harp McGovern and the late P. J. McGovern for their vision and support; F. Zhang for advice and reagents for CRISPR; D. G. Amaral for sharing image resources for creating eye-tracking stimuli; J. Bachevalier for advice on behavior testing; E. A. Murray for guidance on the Wisconsin General Test Apparatus assay; G. Genovese and R. Rosario for support with statistical and bioinformatics analysis; S. Sharma, S. Lall and S. Krol for critical reading of the manuscript; L. Dennis, N. Nien-Chu Espinoza, S. Yang, A. Chakrabarti, N. Joshi and Y. Fukumura for behavioral scoring; X. Wu, X. Ding, L. Cheng and X. Liu for technical support; the veterinary team of Blooming-Spring for excellent colony management and technical support; and S. E. Hyman (Stanley Center for Psychiatric Research, Broad Institute of MIT and Harvard), N. Sanjana (NYU) and L. Cong (Stanford University) and members of the Feng laboratory at MIT for critical discussion on this project. This work was supported by National Key R&D Program of China (2017YFC1307500); Shenzhen Overseas Innovation Team Project (KQTD20140630180249366); Guangdong Innovative and Entrepreneurial Research Team Program (2014ZT05S020). S.Y. and Q.K. was supported by Frontier and Innovation of Key Technology Project in Science and Technology Department of Guangdong Province (2014B020225007 and 2019B020235002); and Program for New Century Excellent Talents in University of Ministry of Education of the People's Republic of China (NCET-12-1078). This work was also supported by the National Key R&D Program of China (2018YFA0107203 and 2017YFA0103802 to A.P.X., 2017YFA0103802 to W.L.); the External Cooperation Program of Chinese Academy of Sciences (172644KYSB20160026); International Partnership Program of Chinese Academy of Sciences (172644KYS820170004 to L.W., 172644KYSB20160175 to H.Z.); the Patrick J. McGovern Foundation; Hundred Talent Program of Chinese Academy of Sciences to H.Z.; the National Natural Science Foundation of China (81425016 to A.P.X., 31671119 to Z.L.); Shenzhen Science and Technology Innovation Commission grants (JCYJ20151030140325151 to H.Z.; GJHZ20160229200136090, JCYJ20170413165053031 to T.Y.; JCYJ20170413162938668 to Z.L.). Y. Zhou was supported by postdoctoral fellowships from the Simons Center for the Social Brain at MIT and Nancy Lurie Marks Family Foundation. G.F. is supported by the McGovern Institute for Brain Research at MIT, James and Patricia Poitras Center for Psychiatric Disorders Research at MIT, the Stanley Center for Psychiatric Research at the Broad Institute of MIT and Harvard, the Hock E. Tan and K. Lisa Yang Center for Autism Research at MIT, and Edward and Kay Poitras. L.W. is also supported by Guangdong Provincial Key Laboratory of Brain Connectome and Behavior 2017B030301017, Shenzhen Discipline Construction Project for Neurobiology DRCSM [2016]1379, and Shenzhen-Hong Kong Institute of Brain Science.

Reviewer information *Nature* thanks Thomas Bourgeron, Michael Platt and the other anonymous reviewer(s) for their contribution to the peer review of this work.

Author contributions G.F., S.Y. and Y. Zhou conceived the study, and R.D., G.F. and H.Z. provided ongoing guidance on the design. S.Y. and A.P.X. oversaw the generation of mutant monkeys. H.Z. oversaw the characterization of mutant monkeys. Y. Zhou carried out CRISPR design and validation. S.Y., Q.K., H.C., Y. Zhou, J.Y., D.X., Y.H. and A.P.X. generated mutant monkeys. Y. Zhou and D.W. designed and performed molecular, protein, sequencing and off-target analyses. R.L., J.S., Y. Zhou, G.F. and R.D. designed and analysed behavioural experiments and MRI assays. H.Z., L.W., Z.L., T.Y., Y. Zou, M.J., W.J., Y.B., W.M., T.A., Y.L., X.L., W.L., L.H., S.A.A. and M.S. participated in the design or execution of some of the behavioural experiments. R.L., D.S.H., J.W.F. III, J.B.H., A.F.-K., O.M. and S.P. managed and performed behavioural scoring. Y. Zhou, R.L., R.D., J.S. and G.F. wrote the manuscript with input from all authors.

Competing interests The authors declare no competing interests.

Additional information
Extended data is available for this paper at https://doi.org/10.1038/s41586-019-1278-0.
Supplementary information is available for this paper at https://doi.org/10.1038/s41586-019-1278-0.
Reprints and permissions information is available at http://www.nature.com/reprints.
Correspondence and requests for materials should be addressed to H.Z., A.P.X., G.F. or S.Y.
Publisher's note: Springer Nature remains neutral with regard to jurisdictional claims in published maps and institutional affiliations.